ACS Partner Journal

CHEMICAL & BIOMEDICAL IMAGING

pubs.acs.org/ChemBioImaging

Perspective

Advances in Super-resolution Stimulated Raman Scattering Microscopy

Published as part of Chemical & Biomedical Imaging special issue "Sub-diffraction Chemical Imaging".

William J. Tipping,* Karen Faulds, and Duncan Graham*

Cite This: https://doi.org/10.1021/cbmi.4c00057

Read Online

ACCESS | Metrics & More | Article Recommendations

ABSTRACT: Super-resolution optical imaging overcomes the diffraction limit in light microscopy to enable the visualization of previously invisible molecular details within a sample. The realization of super-resolution imaging based on stimulated Raman scattering (SRS) microscopy represents a recent area of fruitful development that has been used to visualize cellular structures in three dimensions, with multiple spectroscopic colors at the nanometer scale. Several fundamental approaches to achieving super-resolution SRS imaging have been reported, including optical engineering strategies, expansion microscopy, deconvolution image analysis, and photoswitchable SRS reporters as methods to break the diffraction limit. These approaches have enabled the visualization of biological structures, cellular interactions, and dynamics with unprecedented detail. In this Perspective, an overview of the current strategies and capabilities for achieving super-resolution SRS imaging will be highlighted together with an outlook on potential directions of this rapidly evolving field.

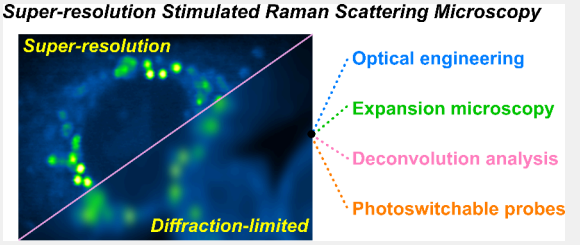

KEYWORDS: *stimulated Raman scattering microscopy, structure−function relationships, super-resolution imaging, photoswitchable probes*

INTRODUCTION

Optical microscopy techniques have proven indispensable for studying the structure−function relationships of a diverse array of specimens within biology, medicine, and chemistry. The diffraction limit as defined by Abbe restricts the spatial resolution to hundreds of nanometers when visible light sources are used for optical microscopy.[1] Super-resolution imaging techniques have been designed to break the diffraction limit and hence provide a nanoscopic view of a sample.[2] Fluorescence-based techniques for surpassing the diffraction limit are widely reported;[3] techniques including structured illumination microscopy (SIM) and stimulated emission depletion (STED) achieve super-resolution imaging through sophisticated excitation patterns, while stochastic optical reconstruction microscopy (STORM), photoactivated localization microscopy (PALM), and Reversible Saturable Optical Fluorescence Transitions (RESOLFT) rely on activation and time-resolved localization of photoswitchable fluorophores to construct a super-resolution image.[4] A fundamental limitation of many fluorescence-based techniques for super-resolution imaging is the requirement for a fluorescent label (e.g., a fluorescent stain or protein) in order to generate imaging contrast. Such labeling results in unavoidable perturbation to the biological system, often with unknown consequences.

Vibrational spectroscopic imaging based on infrared absorption or Raman scattering processes is a group of methods which offer a promising alternative to fluorescence-based techniques because they allow chemically specific detection based on molecular vibrations inherent to the sample. Moreover, to improve the signal-to-noise ratio, vibrational tagging strategies have been developed for miniaturized labeling of many small molecules.[5] For example, alkynes, nitriles, and B−H bonds have been successfully applied to Raman imaging in the cell-silent window (1800−2800 cm^{-1}).[6] As a complementary imaging modality to fluorescence microscopy, stimulated Raman scattering (SRS) microscopy is emerging as a powerful technique for chemical and biomedical imaging applications.[7]

SRS is a form of coherent Raman scattering that uses two synchronized pulsed lasers, known as the pump and Stokes beam, which have different wavelengths and are spatially and temporally overlapped. When the energy difference between the two beams is matched to the Raman transition energy of the chemical bond of interest in the sample, an SRS signal is generated that is enhanced via stimulated emission. A key advantage of SRS imaging is the potential for fast acquisition

Received: July 24, 2024
Revised: September 16, 2024
Accepted: September 20, 2024

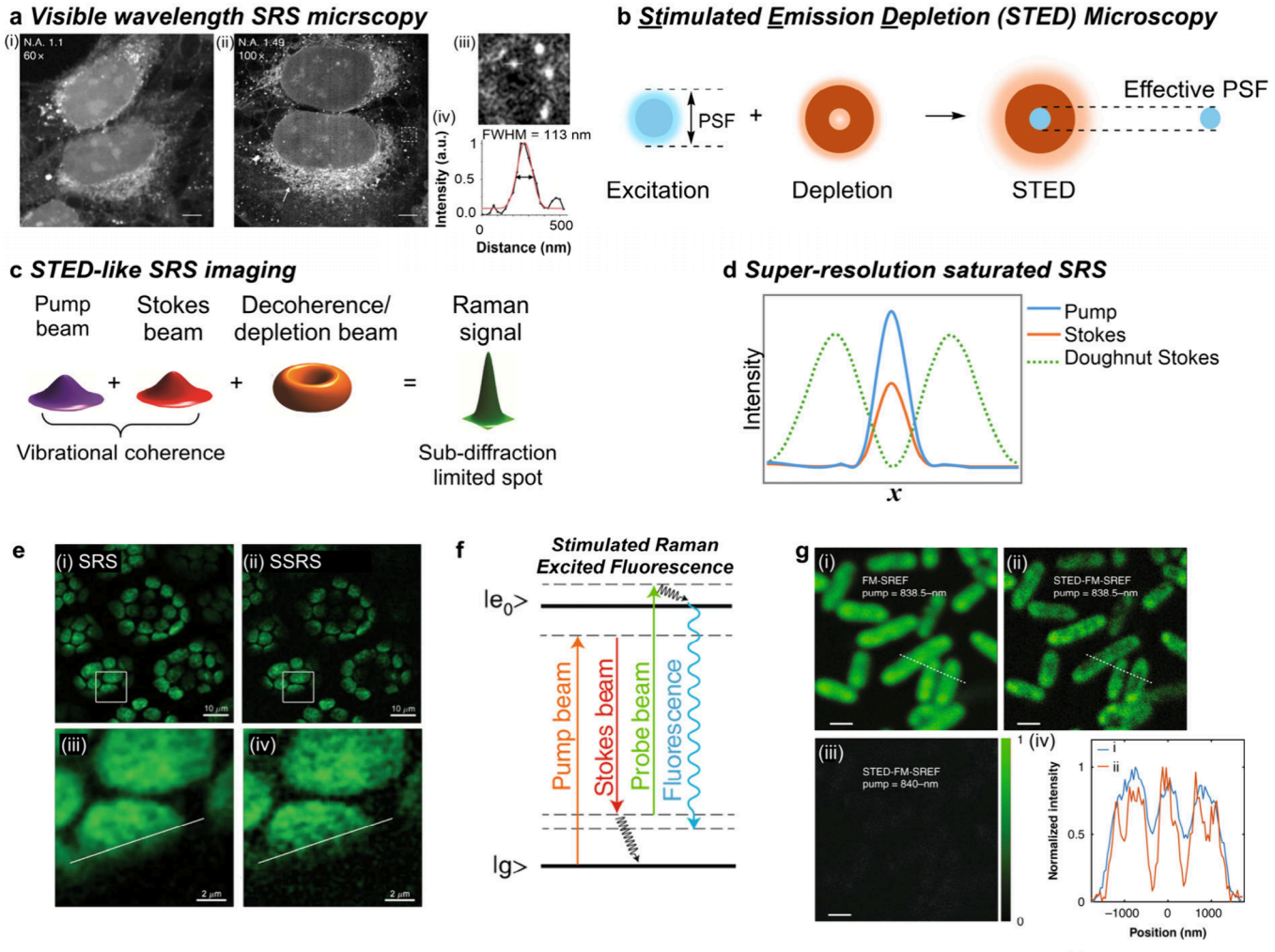

Figure 1. Optical engineering strategies to improve spatial resolution of SRS imaging across various biological samples. (a) Direct comparison of NIR and Visible SRS imaging in U-2 OS cells. SRS images were acquired using (i) NIR lasers at 800 and 1040 nm or (ii) visible lasers at 450 and 520 nm. (iii) Expanded view of the region identified by the white dashed marker in (ii). (iv) Intensity profile of a lipid droplet in (iii) with a full width half maximum (FWHM) of 113 nm. Scale bars: 5 μm. Image reproduced from ref 11 under CC BY license. (b) Stimulated emission depletion (STED) microscopy. In conventional STED microscopy, an excitation beam is overlapped with a depletion (or decoherence) beam of doughnut shape, which reduces the point-spread-function (PSF), thus improving the spatial resolution. (c) Schematic of STED-like SRS imaging. A pump and Stokes (purple and red, respectively) pulse interact with the sample to create vibrational coherence. A spatially shaped decoherence beam (orange) destroys the vibrational coherence in the ring region to leave a residual SRS signal generated at the center region (green). Image adapted and reproduced from ref 16 with permission from the American Chemical Society. (d) Intensity profiles of the three beams at the focal plane after a microscope objective for super-resolution saturated SRS microscopy. *X* is the lateral coordinate on the focal plane. Image adapted and reproduced from ref 14 with permission from the American Physical Society. (e) Comparison of (i) conventional SRS microscopy and (ii) super-resolution saturated SRS (SSRS) microscopy of chloroplasts in leaf sheath cells of rice. Expanded views of the selected area in the dashed marker are provided in parts (iii) and (iv), respectively. SRS imaging was performed at 1530 cm^{-1} (chlorophyll-*a*, -*b* and -*d* modes). Images adapted and reproduced from ref 15. with permission from the American Physical Society. (f) Energy diagram for stimulated Raman excited fluorescence (SREF). Reproduced from ref 7. with permission from Springer Nature. (g) Super-resolution SREF imaging of *E. coli* treated with rhodamine 800. The pump wavelength was set to 838.5 nm corresponding to the nitrile (C≡N) band of rhodamine 800 under (i) frequency modulated (FM) SREF and (ii) STED-FM-SREF. An off-resonance image is provided in (iii), while an intensity line-plot is presented in (iv) across the dashed white line in (i) and (ii), respectively. Scale bars: 1 μm. Images adapted and reproduced from ref 21 under CC BY license with permission from Springer Nature.

and label-free detection of cellular biomolecules based on inherent molecular vibrations. The label-free imaging capability of SRS microscopy is a competitive advantage of the technique, especially given the spectral discrimination of biomolecular signatures that can be probed by using Raman scattering techniques. In addition, the potential for multiplex detection of numerous intracellular targets can be achieved by fine-tuning the vibrational resonances of bio-orthogonal tags to expand the color palette,[8] or through the use of innovative signal enhancement regimes, including electronic preresonance (EPR) SRS,[9] where the absorption wavelength of the reporter molecule approaches that of the incident pump laser wavelength used for SRS imaging. Combined, SRS imaging enables fast acquisition and high content microscopy of multiple cellular targets in a labeled or label-free measurement.

Since the first report of SRS microscopy for live-cell imaging in 2008,[10] the technique has gained significant traction for biological imaging. Key to the success of SRS imaging is label-

https://doi.org/10.1021/cbmi.4c00057
Chem. Biomed. Imaging XXXX, XXX, XXX−XXX

free detection coupled with a narrow bandwidth associated with Raman transitions for multiplex detection in live-cell systems. Most SRS microscopes use near-infrared (NIR) lasers as the incident light sources, employing a tunable pump beam (typically a tunable optical parametric oscillator (OPO) across the range 700−990 nm) and a fixed Stokes beam (typically a fixed wavelength laser at 1031, 1041, or 1064 nm). As such, the lateral spatial resolution is described by the Rayleigh criterion, which is restricted to ∼300 nm under these experimental conditions. Notwithstanding the progress that has been achieved using SRS microscopy for chemical and biomedical imaging applications, the development of super-resolution imaging represents a recent and burgeoning area of development. Key to the success of super-resolution SRS imaging is the ability to perform label-free detection of biochemical species under biocompatible imaging conditions. Recent strategies are beginning to develop super-resolution imaging based on SRS microscopy to drive applications in biological and materials characterization. This Perspective highlights the four main areas of development that have enabled super-resolution SRS imaging, including the development of (i) innovative optical engineering strategies, (ii) the application of expansion microscopy, (iii) the use of deconvolution analysis to improve the lateral spatial resolution, and (iv) the development of optical reporters and photoswitchable motifs for super-resolution SRS imaging. This will provide an overview of the current technical developments and a summary of the remaining challenges together with the potential future advances that will drive super-resolution SRS imaging for chemical and biomedical imaging applications.

OPTICAL ENGINEERING STRATEGIES TOWARD SUPER-RESOLUTION IMAGING

Pushing the Spatial Resolution of Diffraction-limited SRS Microscopy

Given that the spatial resolution of optical imaging is dependent upon the wavelength of the incident light source, an innovative method to directly improve the lateral spatial resolution for SRS microscopy was demonstrated by Bi et al., who employed visible-wavelength lasers for imaging.[11] By incorporating two beta-barium borate (BBO) crystals into the optical design, the NIR wavelengths of the pump and Stokes beams were reduced by half to 450 and 520 nm, respectively. In doing so, the theoretical spatial resolution of the visible-wavelength SRS setup was determined to be 130 nm, enabling label-free imaging in cultured neurons, brain tissue sections and mammalian cells (Figure 1a). An extension of this method coupled visible-wavelength SRS microscopy to electronic preresonance SRS imaging[9] for improved detection sensitivity. In this work, Zhuge et al. demonstrated visible wavelength SRS microscopy of retinoids, which produce a peak maximum absorption at ∼325 nm, that resulted in an increased detection sensitivity via electronic preresonance enhancement.[12] Frequency doubling of the NIR laser wavelengths (at 964 and 1045 nm) using a BBO and a lithium triborate (LBO) crystal generated visible pump and Stokes beams at 482 and 522.5 nm, respectively. Given that the pump wavelength is close to the peak maximum of the absorption profile for retinoids (∼325 nm), a preresonance enhancement of the retinoid signal was generated. These methods are not super-resolution by definition of breaking the diffraction limit of the optical setup; however, currently these studies represent the highest spatial resolution for diffraction-limited SRS imaging to date. A challenge of using visible wavelengths for SRS microscopy is the increased potential for phototoxicity associated with higher energy, shorter wavelength lasers. However, these reports demonstrate the potential for improving the lateral spatial resolution of SRS microscopy by using visible laser wavelengths to do so.

STED-based Approaches for SRS Microscopy

A variety of optical engineering techniques have been developed for super-resolution imaging, of which stimulated emission depletion (STED) is a leading example. In fluorescence microscopy, STED can achieve sub-50 nm spatial resolution through the use of a dual laser irradiation scheme. To do so, the coalignment of a Gaussian excitation beam, used for fluorophore excitation, and a second STED beam—sometimes referred to as a decoherence or depletion beam—is tuned in wavelength to de-excite fluorophores via stimulated emission (Figure 1b).[13] A doughnut-shaped STED beam is typically used because it has a focal intensity distribution with a zero intensity in the center of the beam profile. As such, only fluorophores located at the very center are detected via the Gaussian beam, while the STED beam depletes almost all emission laterally, leaving only the focal Gaussian spot with a dimension that is below the diffraction limit. Hence, this configuration reduces the effective point-spread function (PSF) of the Gaussian beam, enabling a super-resolution measurement. When applied to super-resolution SRS imaging, a doughnut-shaped "STED-like" beam to suppress the Raman signal in a predefined area is the most commonly used method (Figure 1c). Gong et al. first proposed saturated SRS (SSRS) microscopy in 2014, whereby a doughnut-shaped Stokes beam is introduced to make stimulated Raman loss (SRL) signal saturated at the rim of the focal spot, therefore, upon application of an additional Gaussian Stokes beam, the detected SRL signal is confined in a small area defined by the doughnut-shaped Stokes beam (Figure 1d).[14] In a follow-up report, the group experimentally confirmed the subdiffraction limit imaging capability of saturated SRS in chloroplasts (Figure 1e) and live HeLa cells, demonstrating a resolution enhancement factor of 1.41.[15] Another early demonstration of a STED-like detection scheme for super-resolution SRS imaging was in 2015.[16] In this work, a picosecond (ps) pump beam at 800 nm and a broadband femtosecond (fs) probe beam (830−1000 nm) were used to generate a Gaussian-shaped SRS signal. An additional doughnut-shaped decoherence beam at 800 nm was used to turn off the SRS signal at the outer edge of the Gaussian-shaped SRS beam, thereby improving the spatial resolution close to 2-fold when scanning the edge of a Raman-active diamond. Würthwein et al. demonstrated that a 2-fold resolution enhancement could be achieved in saturated femtosecond SRS imaging.[17] The configuration was simplified though the use of only two wavelength components: a femtosecond Stokes beam and depletion beam at 1030 nm, and a pump beam tunable across the range 780−1000 nm. In an analogous approach, Kim et al. carried out three-beam SRS measurements employing a picosecond (ps) pump beam, a fs Stokes beam and a ps depletion beam which were spatially and temporally overlapped.[18] This system was used to image the Raman-active modes of benzene at 992 cm^{-1} (ring breathing mode) and 3062 cm^{-1} (C−H stretching mode). In these early examples of suppression SRS microscopy, the potential for

https://doi.org/10.1021/cbmi.4c00057
Chem. Biomed. Imaging XXXX, XXX, XXX−XXX

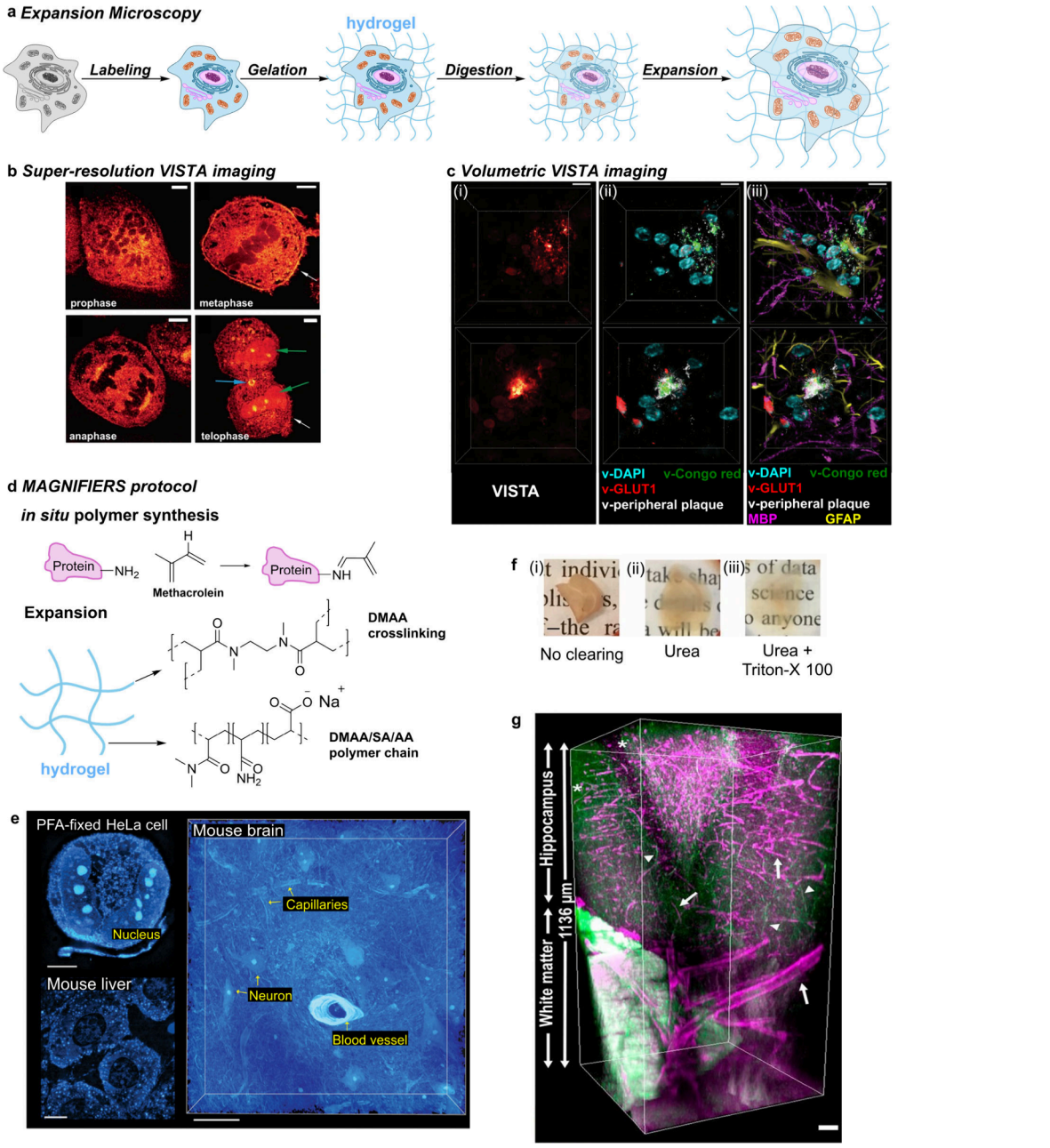

Figure 2. Super-resolution SRS imaging using expansion microscopy and tissue clearing methods. (a) General procedure for sample preparation in expansion microscopy. (b) Super-resolution VISTA imaging of mitotic HeLa cells using the 2940 cm^{-1} stretch (CH_3 stretch) for contrast. Scale bars: 20 μm. Images adapted and reproduced from ref 23 under CC BY license with permission from Springer Nature. (c) VISTA imaging of amyloid-β plaque in a mouse brain sample (2 replicates). (i) VISTA imaging was performed at 2940 cm^{-1} (CH_3 stretch) together with (ii) a four-channel overlay for v-DAPI (cyan, nuclei), v-Congo red (green, for plaque core), v-GLUT1 (red, blood vessels), and v-peripheral plaque (white) by U-net-predicted high-resolution segmentation of the VISTA images in (i). (iii) Six-color tandem fluorescence image of MBP (magenta, myelin basic protein) and GFAP (yellow, glial fibrillary acidic protein) with 4-channel VISTA predictions. Scale bars: 30 μm. Image reproduced from ref 24 with permission from the Royal Society of Chemistry. (d) Super-resolution SRS imaging of biological samples using MAGNIFIERS expansion. Abbreviations: acrylamide (aa), sodium acrylate (SA) and *N*,*N*-dimethylacrylamide (DMAA). (e) Using the MAGNIFIERS protocol, 3D-rendered SRS images at 2941 cm^{-1} (CH_3 vibration) of PFA-fixed HeLa cell with expansion factor (EF) = 4.5, and mouse brain (EF = 4.5) and mouse liver (EF = 4.3) are presented. Scale bars: 10 μm. Images adapted and reproduced from ref 26 with permission from Wiley-VCH GmbH. (f) Photographs of 1 mm thick brain slices in (i) PBS, (ii) cleared with 8 M urea, and (iii) 8 M urea containing 0.2% Triton X-100. Scale bars: 2 mm. (g) Volumetric reconstruction of the hippocampus and white matter in mouse brain tissue. Scale bar: 50 μm. Images in (f) and (g) are reproduced from ref 27 with permission from the National Academy of Sciences.

subdiffraction limit chemical imaging was demonstrated. A remaining challenge for these early approaches is their application to biological systems, where the detected SRS signals are typically weaker than those detected from neat solvents.

A particular challenge for the widespread application of STED-like SRS imaging is the complex optical designs required to do so, which may restrict these methods to specialized laboratories. That being said, fluorescence-based STED microscopes have achieved commercial success,[19] demonstrat-

https://doi.org/10.1021/cbmi.4c00057
Chem. Biomed. Imaging XXXX, XXX, XXX−XXX

ing the potential opportunities for an SRS-based alternative. A second major challenge associated with STED-like SRS imaging is the insensitive nature of Raman scattering, particularly when such illumination schemes achieve super-resolution excitation from a subdiffraction limited focal spot. Thus, the reported super-resolution vibrational imaging methods are usually based on excitation saturating or excitation depleting conditions, which require extremely intense laser power to achieve a moderate resolution improvement. Under these conditions, it can limit some biological applications due to phototoxicity. To directly address this issue, Xiong et al. developed Stimulated Raman Excited Fluorescence (SREF) as an ultrasensitive vibrational spectroscopy which combined the chemical specificity of Raman scattering with the sensitivity of fluorescence detection (Figure 1f).[20] In follow up work, the group coupled SREF with STED-like illumination for super-resolution vibrational imaging with high detection sensitivity.[21] Briefly, the SREF relies upon a pump and Stokes beam to coherently populate an intermediate vibrational state by SRS, before a third probe beam is used to upconvert the vibrationally excited population to an electronically excited state for subsequent fluorescence detection. Interestingly, the combination of STED with SREF was unable to achieve super-resolution imaging due to the presence of a parasitic anti-Stokes fluorescence background, which could not be removed by depletion using the STED beam. To overcome this issue, the authors adopted a frequency modulation (FM) scheme, whereby temporal modulation of the excitation frequency on- and off- the target vibrational resonance (but still within the line width of the background) resulted in an intensity modulation of the vibrational signal, but not an intensity modulation of the background. The authors applied the newly created STED-FM-SREF to visualize rhodamine 800 distribution in *Escherichia coli* using the nitrile moiety as a vibrational marker (Figure 1g). A heterogeneous distribution of rhodamine 800 signal in *E. coli* as detected in the super-resolution SREF images, but not in the diffraction-limited images, demonstrated the power of this technique. This report marked several key achievements for super-resolution vibrational imaging. First, the development of FM to overcome the anti-Stokes fluorescence background ultimately lead to super-resolution SREF imaging with biocompatible excitation laser power. Second, because SREF detection improved the detection sensitivity, super-resolution imaging could be achieved with lower laser irradiation power compared to previous methods.

In summary, STED-like SRS imaging has made substantial progress in the visualization of biological features with subdiffraction limit resolution. However, challenges remain regarding this approach, notably the weak scattering efficiency of Raman processes which can result in limited signal intensities detected through this method. Consequently, a modest improvement in the spatial resolution is achieved at the expense of imaging speed and/or incident laser intensity, which can be problematic, particularly for biological samples. While this can pose a challenge, it is one with significant reward, especially given that STED-like SRS can produce super-resolution imaging data from label-free measurments.

EXPANSION SRS MICROSCOPY

Expansion microscopy can achieve nanoscale spatial resolution imaging through physically expanding the sample by embedding it in a swellable polymer network (Figure 2a). In doing so, the biological components within the sample are isotropically separated in space, thereby facilitating their detection using a conventional diffraction-limited optical setup. In addition, tissue clearing methods have been developed in conjunction with expansion microscopy to overcome the opacity and poor penetration of the incident laser source across intact tissue samples. Combined, these approaches have improved the lateral and axial resolution when applied to microscopic imaging based on fluorescence and SRS. At this point, the reader is directed to a recent review which highlights the application of tissue clearing and expansion microscopy to fluorescently labeled biological samples,[22] while the application of expansion microscopy to SRS imaging is the focus in this section.

The combination of expansion microscopy with SRS imaging was realized by Qian et al. in 2021, who demonstrated three-dimensional SRS imaging with a resolution of 78 nm in HeLa cells.[23] The method was termed *vibrational imaging of swelled tissues and analysis* (VISTA) in which biological samples were embedded in a polymer hydrogel, before expansion of the sample-hydrogel hybrid in water, and SRS visualization of retained CH_3 groups, indicative of endogenous proteins. VISTA was shown to be capable of label-free super-resolution imaging of the endogenous protein distribution throughout cellular division (Figure 2b). The VISTA platform was validated against immunofluorescent markers in murine brain tissue samples before multicomponent imaging of hippocampal brain tissue was performed. The same grouping extended the VISTA platform to visualize protein aggregates in neurodegenerative disease models,[24] together with the development of machine learning image segmentation to augment the label-free SRS imaging of mouse brain tissue.[25] The combination of the U-NET machine learning algorithm, with ground truth immunofluorescence, meant the VISTA platform was capable of predicting the location of the nucleus, blood vessels, neuronal cells, and dendrites in murine brain tissues with high accuracy (Figure 2c).

To expand the range of biomolecules amenable to expansion SRS microscopy, Shi et al. developed *molecule anchorable gel-enabled nanoscale Imaging of Fluorescence and stimulated Raman scattering microsc*opy (MAGNIFIERS).[26] The use of methacrolein and heat denaturation replaced the use of 6-((acroyl)amine) hexanoic acid and proteinase *k* digestion to substantially improve the retention of protein components prior to sample expansion (Figure 2d). Under these milder conditions, sub-50 nm resolution was achieved using SRS in combination with fluorescently labeled substrates in tissue and organoid samples. An attractive feature of MAGNIFIERS was the compatibility of the method across a variety of biological samples, including cells and tissues from which the endogenous protein content was visualized using SRS imaging at 2941 cm^{-1} (CH_3 stretching mode) (Figure 2e).

Tissue clearing methods have been applied to SRS imaging applications and have largely been used to improve the axial imaging resolution. Wei et al. developed formulations of 8 M urea or 8 M urea supplemented with 0.2% Triton X-100 as Raman-compatible tissue clearing solutions (Figure 2f).[27] In doing so, a 10-fold improvement in axial imaging depth was achieved in cleared tissue samples, including murine hippocampal sections (Figure 2g). The group also demonstrated that using these reagents, the method resulted in the retention of lipid and protein components, as observed in the hyperspectral SRS imaging of tissue and spheroid samples. The approach was

https://doi.org/10.1021/cbmi.4c00057
Chem. Biomed. Imaging XXXX, XXX, XXX−XXX

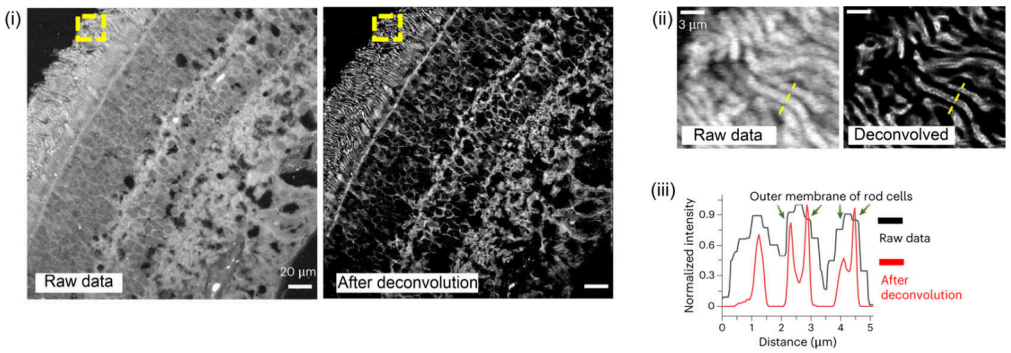

Figure 3. Super-resolution SRS imaging using deconvolution image analysis. Super-resolution SRS imaging of a human retinal section using A-PoD. (i) SRS images acquired at 2930 cm^{-1} (raw data) prior to deconvolution using A-PoD (after deconvolution). (ii) Expanded view of the region identified by the yellow marker in (i). (iii) An intensity plot shows the resolution enhancement afforded by A-PoD. Images adapted and reproduced from ref 31 with permission from Springer Nature.

augmented using spectral phasor analysis[28] which enabled the segmentation of various components of brain image slices into the constituent biological regions of interest, including the axons, cellular nuclei and vasculature. To further improve the detection sensitivity when applied to tissue clearing SRS microscopy, Shi et al. created a tissue clearing platform termed RADIANT: *Raman Dye Imaging and Tissue Clearing*, which was compatible with electronic preresonance Raman dyes for high-content multicomponent imaging using SRS microscopy.[29] RADIANT imaging was shown to enable the detection of 11 intracellular targets in brain slices >1 mm thick, thereby extending the imaging depth by 10- to 100-fold compared to previous multiplex imaging methods.

In summary, a general challenge for expansion microscopy and tissue clearing methods is their incompatibility with living samples. In addition, the use of some of the reagents outlined above results in the loss of biomolecular components, in particular, cellular lipids. The development of expansion microscopy and tissue clearing with enhanced lipid retention will further increase the applicability of these methods for biological imaging. As these methods do not require a reconfiguration of the optical design, there exists significant potential for the application of these techniques using commercial SRS microscope systems. Furthermore, expansion microscopy methods retain the precise chemical specificity of the sample that can be effectively imaged using label-free SRS.

■ DECONVOLUTION ANALYSIS

Image deconvolution analysis refers to computational methods that remove image distortion and, subsequently, improve the spatial resolution of the image. Distortion in optical microscopy results in an image that is blurred by light diffraction; the blurring effect can be modeled and expressed by a point-spread-function (PSF). Thus, by modeling the PSF associated with the blurring and combining the model with a suitable deconvolution algorithm, enhancement in the spatial resolution of microscopic images can be achieved. A wide variety of deconvolution algorithms have been developed for this purpose.[30] The application of image deconvolution analysis to computationally improve the resolution of SRS images is a relatively recent development. A prominent example developed super-resolution imaging based on Adam-based pointillism deconvolution (A-PoD) to improve the spatial resolution of SRS images to 50−100 nm (Figure 3).[31] This approach mimics the concept of pointillism painting and describes images as multiple discontinuous spots (referred to as virtual emitters).[32] The virtual emitters have the same unit intensity, and the total number of emitters is fixed. This characteristic allowed for suppression of imaging artifacts. Consequently, from low-resolution images containing a high density of emitters, super-resolution images may be restored. Using A-PoD, the authors demonstrated three-dimensional, super-resolution imaging in HeLa cells, together with metabolic imaging enabled through D_2O culture in *drosophila* brain samples, and label-free super-resolution imaging of human retinal sections (Figure 3). The method was also shown to be compatible with multimodal super-resolution imaging by combining fluorescence and SRS microscopy on the same sample: HEK293 cells were labeled with Mito-RFP, a red fluorescent protein to visualize the mitochondrial distribution, while SRS imaging of the protein and lipid pools were visualized at 2930 and 2850 cm^{-1}, respectively. This method provided molecularly specific information at a spatial resolution of less than 59 nm on a single lipid droplet. The wider potential of super-resolution SRS imaging using A-PoD is likely to be realized through metabolic imaging studies where label-free visualization is a significant advantage.

In an alternative approach, Gong et al. used the Richardson−Lucy (RL) deconvolution method to realize a 2.2-fold improvement in the spatial resolution as an alternative strategy achieve super-resolution SRS imaging.[33] The grouping paired a squeezed light illumination scheme to reduce the shot noise of the laser with RL deconvolution analysis to perform super-resolution SRS imaging of porcine muscle. SRS imaging of porcine muscle tissue was performed using the 2894 cm^{-1} mode (CH_3 stretching) indicative of the protein and lipid content. These early studies indicate the potential for deconvolution image analysis applied to SRS microscopy to computationally improve the imaging resolution. In that way, deconvolutional analysis negates the requirement for modification to the optical path to enable super-resolution imaging in a way that offers potential accessibility to wide-field microscope setups. In addition, the analysis is performed after image capture and, therefore, extends the computability of the technique across sample types and a broad diversity of vibrational resonances. Although the field of deconvolution super-resolution microscopy is rapidly evolving, due caution must be exercised regarding the potential for AI-generated image artifacts. Innovative solutions to this issue are actively being developed and would be recommended to mitigate the risk of overprocessing imaging data, which will be particularly

https://doi.org/10.1021/cbmi.4c00057
Chem. Biomed. Imaging XXXX, XXX, XXX−XXX

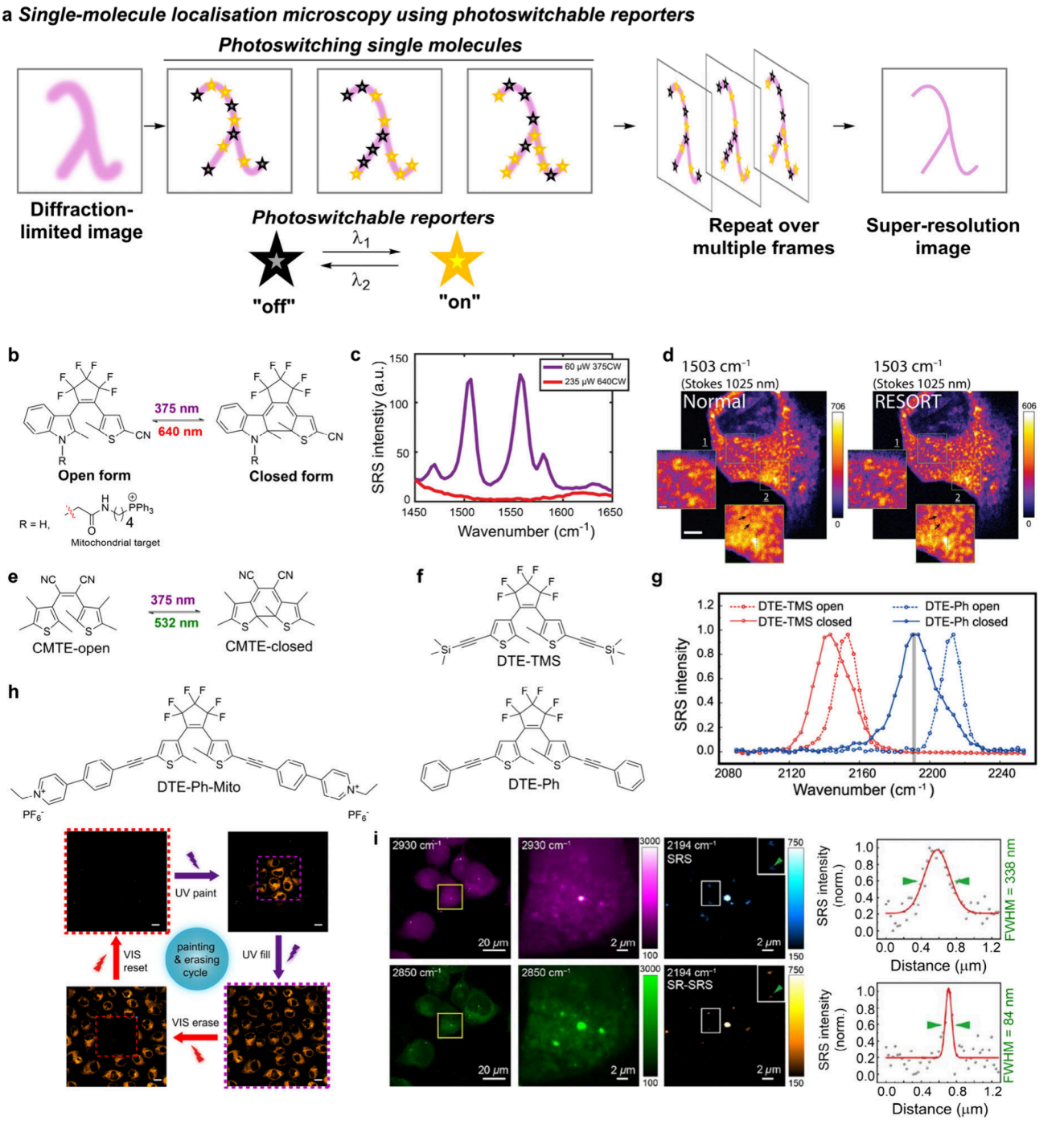

Figure 4. Application of photoswitchable probes for super-resolution SRS imaging. (a) Principle of single-molecule localization microscopy. Individual photoswitchable probes are detected with high positional certainty in a sequential fashion by alternating between an "on" and "off" state. The acquisition of many frames each containing a sufficiently sparse subset of reporters in the "on" configuration allow the detection of individual probes. (b) Molecular structure of DAE photoswitch that is responsive to UV and red laser activation between the closed and open forms, respectively. (c) SRS spectrum of DAE photoswitch (R═H) presented in (b) following UV (375 nm CW) or red (640 nm CW) laser irradiation. (d) Super-resolution SRS imaging of a DAE photoswitch containing a mitochondrial targeting group (as shown in (b)) under normal SRS and RESORT microscopy conditions in fixed HeLa cells. Figures in (b–d) adapted and reproduced from ref 36. with permission from the American Association for the Advancement of Science. (e) Molecular structure of the open and closed forms of the photoswitch, CMTE. (f) Molecular structures of the open forms of the photoswitches DTE-TMS and DTE-Ph. (g) SRS spectra of DTE-TMS and DTE-Ph in the open- and closed-ring forms. (h) Molecular structure of DTE-Ph-Mito together with HeLa cell "painting" and "erasing" cycle based on the photoswitching of DTE-Ph-Mito using controlled UV/visible irradiation in the areas marked by the purple and red dashed squares. Scale bar: 20 μm. Figures in (f–h) are adapted and reproduced from ref 39 with permission from Springer Nature. (i) Super-resolution SRS microscopy was performed using the photoswitchable DTE-Ph-NPs in live HeLa cells. SRS images were acquired at 2930 and 2850 cm^{-1} (CH_3 and CH_2 stretch, respectively), together with 2194 cm^{-1} (C≡C, closed ring isomer) under diffraction limited (SRS) and super-resolution (SR-SRS) imaging conditions. SRS signal intensity of the 2194 cm^{-1} images was measured with a Gaussian function to determine the fwhm (green arrows). Images adapted and reproduced from ref 40 with under CC BY license. Copyright the authors.

https://doi.org/10.1021/cbmi.4c00057
Chem. Biomed. Imaging XXXX, XXX, XXX−XXX

important when analyzing complex biological environments. Given the diversity of deconvolution analysis approaches that have been created, together with advances in machine learning and artificial intelligence for image analysis,[34] it is anticipated that this area has much potential for future growth and development.

PHOTOSWITCHING SRS MICROSCOPY

Single-molecule localization microscopy (SMLM) is most commonly applied to the precise localization of photoswitchable fluorescent reporters (Figure 4a).[35] The technique relies upon the premise that the spatial location of single fluorescent molecules can be determined if the PSFs do not overlap. To do so, the fluorescent emission of individual fluorophores are separated in time; photoswitching is the most common technique to achieve this aim, whereby the fluorescent molecule can switch between an active "on" state, thus emitting fluorescence, and an inactive "off" state where it does not fluoresce. This process is exemplified in reversible saturable optical fluorescence transition (RESOLFT) microscopy. SMLM has been achieved by using photoswitchable Raman reporters to enable super-resolution SRS imaging. This relatively new detection scheme relies upon the development of Raman reporters that produce a shift in the spectroscopic properties upon irradiation with a continuous wave (CW) laser. Several groups have developed photoswitchable Raman reporters for SRS microscopy which can be switched between two distinct isomers by irradiation with ultraviolet or visible light, thus turning the Raman signal "on" or "off". The design and application of photoswitchable reporters for super-resolution SRS imaging are emerging and are discussed in detail below.

Shou et al. developed diarylethene (DAE) photoswitches containing a pendant nitrile group for detection in the cellular-silent region under a RESOLFT-like irradiation scheme (Figure 4b). Here, the authors used a pump and Stokes beam for SRS imaging, a UV beam for activation of the photoswitch and a doughnut-shaped depletion beam to improve the PSF.[36] This process was referred to as reversible saturable optical Raman transitions (RESORT) microscopy. Under CW irradiation using a 375 nm laser, the closed form of the DAE photoswitch produced prominent SRS peaks at 1503 and 1557 cm^{-1} (Figure 4c), while a weaker signal was detected at 2217 cm^{-1} indicative of the nitrile group. Following irradiation with a 640 nm CW laser, the open form of the DAE was produced, resulting in the loss of the aforementioned peaks. As such, in live HeLa cells, the SRS signal was successfully photoswitched by alternately applying a UV 375 nm CW laser and a doughnut-shaped 640 nm CW laser, pushing the spatial resolution to 151 nm. Incorporating a triphenyl phosphonium targeting group into the molecular design (Figure 4b) enabled super-resolution SRS imaging of mitochondria in fixed HeLa cells (Figure 4d). In a related work, Shou et al. demonstrated the potential of *cis*-1,2-dicyano-1,2-bis(2,4,5-trimethyl-3-thienyl)ethene, (CMTE, Figure 4e) for photoswitching following UV irradiation.[37] Despite the presence of two nitrile groups in CMTE, photoswitching was followed using the intensity of a Raman mode at 1510 cm^{-1} upon irradiation at 375 nm to generate the closed form of CMTE. As an early example of photoswitching SRS microscopy, this work demonstrated the feasibility of the technique, but conceded that the signal-to-noise could be improved using a bio-orthogonal tagging strategy[38] based on alkynes. To demonstrate the potential of that strategy, Ao et al. developed a suite of photochromic dithienylethene (DTE) analogues containing alkyne functional groups for detection in the cell-silent region of the Raman spectrum.[39] The group expanded the color palette for photoswitchable SRS imaging by creating different spectroscopic colors through end-capping of the alkyne group with trimethylsilyl (DTE-TMS, $\nu_{C\equiv C}$ = 2154 cm^{-1}) and phenyl (DTE-Ph, $\nu_{C\equiv C}$ = 2214 cm^{-1}) substituents (Figure 4f, g). Under UV irradiation, a photoisomerization process was shown to occur and the resulting ring-closing reaction altered the electronic structure and red-shifted the absorption spectra of the DTE units. In doing so, a large Raman frequency shift of the conjugated alkyne group also resulted (Figure 4g), together with an enhancement in the SRS scattering intensity via EPR-SRS effects. The authors demonstrated that it was possible to use the photoswitch DTE-Ph-Mito for painting and erasing cycles based on UV and visible laser irradiation (Figure 4h). In order to achieve subdiffraction limit resolution for SRS microscopy, the group included an ultraviolet activation beam for the DTE-Ph photoswitch together with a depletion beam of doughnut shape to confine the PSF of SRS detection.[40] To demonstrate super-resolution SRS imaging using this method, the group prepared polystyrene-based nanoparticles (NPs) that were doped with a DTE-Ph photoswitch (DTE-Ph NPs). In HeLa cells treated with the DTE-Ph NPs, a 4-fold improvement in spatial resolution to ∼84 nm was achieved (Figure 4i). In a complementary method, Yang et al. demonstrated multiplex photoswitching by coupling asymmetric DAE structures with the supermultiplexed *Carbow palette*[41] to detect up to 16 photoswitchable Raman frequencies.[42] By incorporating heterocycle modification, end-capping substitutions, and isotopic editing of the alkyne groups contained within the DAE polyynes, tuning of the electronic and vibrational spectra was feasible. This recent study highlights the potential for multiplex photoswitchable SRS imaging, albeit under diffraction-limited conditions at present. The application of these unique probes for super-resolution SRS imaging is likely to represent a fruitful area of development. Further examples for achieving photoswitching based on electronic preresonance enhancement to improve detection sensitivy,[43] and photoactivatable Raman probes based on the photoconversion of cyclopropenones to alkynes have also been reported;[44] the application of these techniques to super-resolution SRS imaging are also keenly anticipated.

In summary, these early examples have reported unique molecular photoswitches that are compatible with super-resolution SRS imaging within cells. With the narrow resonances associated with Raman reporters, the potential of multiplex photoswitches could have far-reaching consequences for imaging. It is worth noting that the use of a photoswitchable reporter does sacrifice the label-free imaging aspect of SRS, and the use of UV irradiation of light activation is known to be cell damaging. However, the expansion of the color palette of photoswitchable reporters is anticipated, together with activation based on visible and infrared laser irradiation would also help to increase to biocompatibility of this approach for super-resolution SRS imaging applications. Targeting the cell-silent region of the Raman spectrum is an important method in vibrational spectroscopic labeling and imaging, and when combined with label-free imaging of the cellular contents in the fingerprint and high wavenumber

https://doi.org/10.1021/cbmi.4c00057
Chem. Biomed. Imaging XXXX, XXX, XXX−XXX

Table 1. Key Advantages and Challenges Associated with the Current Methods for Super-resolution SRS Imaging

Method	Key advantages	Key challenges
STED-like excitation	• Functions with both label-free and labeled SRS imaging experiments	• Complex optical configuration required
	• Significant improvements in spatial resolution can be achieved in living samples	• Weak Raman signals can limit the improvement in spatial resolution • High-power STED lasers can be cell damaging
Expansion microscopy	• Accessible method for nonspecialized laboratories	• Not compatible with living systems
	• No reconfiguration of the optical setup	• The retention of some cellular biomolecules is challenging due to the use of harsh reagents
	• Compatible with multiple sample types	
Deconvolution image analysis	• Direct, label-free imaging without microscope reconfiguration	• The potential for AI-generated image artifacts
	• Adaptable to any sample type	• Some algorithms are computationally slow
Single-molecule localization analysis	• Multiplex super-resolution detection using bioorthogonal photoswitches	• Repetitive imaging cycles can reduce sample throughput
	• Significant spatial resolution improvements can be realized	• The sample is intrinsically labeled

region of the spectrum, a powerful super-resolution imaging platform would result.

CONCLUDING REMARKS AND PERSPECTIVES

As a contrast mechanism for chemical and biomedical imaging, SRS microscopy is emerging as a powerful technique due to the ability to perform fast-acquisition imaging of molecular vibrations for label-free visualization of the sample. Four key strategies are being developed for super-resolution SRS imaging as outlined in this article. A summary of the key advantages and challenges associated with each method are summarized in Table 1.

The early successes of SRS microscopy for bioimaging have centered on the ability to perform label-free detection in living biological samples. Future developments in super-resolution SRS microscopy are anticipated to focus on improvements in image acquisition speed, signal-to-noise (particularly at the nanometer scale), and hyperspectral detection. A critical limitation of Raman-based imaging is the detection sensitivity due to the inherently weak Raman scattering signals. The augmentation of super-resolution SRS with bio-orthogonal tags has proven to be highly successful, and further developments in this area will likely increase the utility of the technique for bioimaging applications. The intricate nature of optical illumination paths based on multiple laser pulses across space and time potentially represents a challenge to the adoption of these techniques to nonspecialist laboratories. As an alternative route for super-resolution imaging, the application of deconvolution image analysis has shown promise for computationally improving spatial resolution. Given the diversity of deconvolution analysis techniques that are available and routinely used in other fields (e.g., astronomy), there remains significant scope to develop this area further.

When considering the diversity of reagents and conditions for expansion microscopy as applied to fluorescently labeled substrates, there exists significant potential for further refinement of these methods when applied to super-resolution SRS microscopy. For example, the development of milder reagents and conditions for expansion microscopy and tissue clearing could also improve the retention of a greater diversity of biomolecular functional groups, including lipid species. As lipids are typically highly Raman-active and are widely studied in the SRS imaging literature, milder conditions for expansion microscopy and tissue clearing would be beneficial. A key consideration in the development of new super-resolution SRS imaging strategies is detection under biocompatible conditions. As a potential example, such methods would facilitate super-resolution imaging of dynamic Raman sensors for intracellular processes, including those for pH[45] among many others.

Hyperspectral SRS imaging has also been widely utilized for molecular compositional analysis, and the augmentation of super-resolution RS imaging with hyperspectral imaging is yet to be fully realized. The development and refinement of computational algorithms and machine learning models for interpreting hyperspectral data sets will likely advance the field toward this aim.[46] In addition, the combination of alternative analytical techniques with super-resolution SRS imaging would enable comprehensive sample characterization. For example, the combination of mass spectrometry imaging, which offers enhanced molecular characterization, with SRS microscopy, which could permit high-resolution visualization of the sample, could be used to identify and target areas for investigation using a hybrid analytical approach.[47] The integration of these two techniques could offer metabolic profiling with enhanced spatial resolution and chemical determination to drive fundamental discoveries in biology and medicine. Alternatively, stimulated Raman scattering has been combined with photothermal microscopy for ultrasensitive chemical detection based on the detection of local heating and subsequent refractive index changes at the laser focus.[48] As a recent development, the potential for super-resolution imaging will likely be assessed.

To conclude, the field of super-resolution SRS microscopy is beginning to evolve with the aim of becoming a high-content imaging platform for chemical and biomedical imaging applications. Given the breadth of techniques and methodologies outlined in this Perspective, it demonstrates the versatility and applicability of SRS towards this aim. It is anticipated that super-resolution SRS imaging will find broad utility across the chemical, medical, and biological imaging fields in the future.

AUTHOR INFORMATION

Corresponding Authors

William J. Tipping − *Pure and Applied Chemistry, University of Strathclyde, Technology and Innovation Centre, Glasgow G1 1RD, United Kingdom;* orcid.org/0000-0003-4273-2691; Email: william.tipping@strath.ac.uk

Duncan Graham − *Pure and Applied Chemistry, University of Strathclyde, Technology and Innovation Centre, Glasgow G1 1RD, United Kingdom*; Email: duncan.graham@strath.ac.uk

https://doi.org/10.1021/cbmi.4c00057
Chem. Biomed. Imaging XXXX, XXX, XXX−XXX

Author

Karen Faulds − *Pure and Applied Chemistry, University of Strathclyde, Technology and Innovation Centre, Glasgow G1 1RD, United Kingdom;* orcid.org/0000-0002-5567-7399

Complete contact information is available at: https://pubs.acs.org/10.1021/cbmi.4c00057

Author Contributions

W.J.T. conceptualization; project administration; writing−original draft; writing−reviewing and editing; visualization. K.F. funding acquisition; supervision. D.G. writing−reviewing and editing; funding acquisition; supervision.

Notes

The authors declare no competing financial interest.

■ ACKNOWLEDGMENTS

We thank the University of Strathclyde and the EPSRC (EP/N010914/1) for financial support.

■ REFERENCES

(1) Graefe, C. T.; Punihaole, D.; Harris, C. M.; Lynch, M. J.; Leighton, R.; Frontiera, R. R. Far-Field Super-Resolution Vibrational Spectroscopy. *Anal. Chem.* **2019**, *91*, 8723−8731.

(2) Tang, M.; Han, Y.; Jia, D.; Yang, Q.; Cheng, J.-X. Far-field super-resolution chemical microscopy. *Light Sci. Appl.* **2023**, *12*, 137.

(3) Schermelleh, L.; Ferrand, A.; Huser, T.; Eggeling, C.; Sauer, M.; Biehlmaier, O.; Drummen, G. P. C. Super-resolution microscopy demystified. *Nat. Cell Biol.* **2019**, *21*, 72−84.

(4) Huang, B.; Bates, M.; Zhuang, X. Super-resolution fluorescence microscopy. *Annu. Rev. Biochem.* **2009**, *78*, 993−1016.

(5) Benson, S.; de Moliner, F.; Tipping, W.; Vendrell, M. Miniaturized Chemical Tags for Optical Imaging. *Angew. Chem., Int. Ed.* **2022**, *61*, e202204788.

(6) Dodo, K.; Fujita, K.; Sodeoka, M. Raman Spectroscopy for Chemical Biology Research. *J. Am. Chem. Soc.* **2022**, *144*, 19651−19667.

(7) Hu, F.; Shi, L.; Min, W. Biological imaging of chemical bonds by stimulated Raman scattering microscopy. *Nat. Methods* **2019**, *16*, 830−842.

(8) Qian, N.; Min, W. Super-multiplexed vibrational probes: Being colorful makes a difference. *Curr. Opin. Chem. Biol.* **2022**, *67*, 102115.

(9) Wei, L.; Min, W. Electronic Preresonance Stimulated Raman Scattering Microscopy. *J. Phys. Chem. Lett.* **2018**, *9*, 4294−4301.

(10) Freudiger, C. W.; Min, W.; Saar, B. G.; Lu, S.; Holtom, G. R.; He, C.; Tsai, J. C.; Kang, J. X.; Xie, X. S. Label-Free Biomedical Imaging with High Sensitivity by Stimulated Raman Scattering Microscopy. *Science* **2008**, *322*, 1857−1861.

(11) Bi, Y.; Yang, C.; Chen, Y.; Yan, S.; Yang, G.; Wu, Y.; Zhang, G.; Wang, P. Near-resonance enhanced label-free stimulated Raman scattering microscopy with spatial resolution near 130 nm. *Light Sci. Appl.* **2018**, *7*, 81.

(12) Zhuge, M.; Huang, K.-C.; Lee, H. J.; Jiang, Y.; Tan, Y.; Lin, H.; Dong, P.-T.; Zhao, G.; Matei, D.; Yang, Q.; Cheng, J.-X. Ultrasensitive Vibrational Imaging of Retinoids by Visible Preresonance Stimulated Raman Scattering Microscopy. *Adv. Sci.* **2021**, *8*, 2003136.

(13) Vicidomini, G.; Bianchini, P.; Diaspro, A. STED super-resolved microscopy. *Nat. Methods* **2018**, *15*, 173−182.

(14) Gong, L.; Wang, H. Breaking the diffraction limit by saturation in stimulated-Raman-scattering microscopy: A theoretical study. *Phys. Rev. A* **2014**, *90*, 013818.

(15) Gong, L.; Zheng, W.; Ma, Y.; Huang, Z. Saturated Stimulated-Raman-Scattering Microscopy for Far-Field Superresolution Vibrational Imaging. *Phys. Rev. Appl.* **2019**, *11*, 034041.

(16) Silva, W. R.; Graefe, C. T.; Frontiera, R. R. Toward Label-Free Super-Resolution Microscopy. *ACS Photon.* **2016**, *3*, 79−86.

(17) Würthwein, T.; Irwin, N.; Fallnich, C. Saturated Raman scattering for sub-diffraction-limited imaging. *J. Chem. Phys.* **2019**, *151*, 194201.

(18) Kim, D.; Choi, D. S.; Kwon, J.; Shim, S.-H.; Rhee, H.; Cho, M. Selective Suppression of Stimulated Raman Scattering with Another Competing Stimulated Raman Scattering. *J. Phys. Chem. Lett.* **2017**, *8*, 6118−6123.

(19) Wegel, E.; Göhler, A.; Lagerholm, B. C.; Wainman, A.; Uphoff, S.; Kaufmann, R.; Dobbie, I. M. Imaging cellular structures in super-resolution with SIM, STED and Localisation Microscopy: A practical comparison. *Sci. Rep.* **2016**, *6*, 27290.

(20) Xiong, H.; Shi, L.; Wei, L.; Shen, Y.; Long, R.; Zhao, Z.; Min, W. Stimulated Raman excited fluorescence spectroscopy and imaging. *Nat. Photonics* **2019**, *13*, 412−417.

(21) Xiong, H.; Qian, N.; Miao, Y.; Zhao, Z.; Chen, C.; Min, W. Super-resolution vibrational microscopy by stimulated Raman excited fluorescence. *Light Sci. Appl.* **2021**, *10*, 87.

(22) Zhang, Y.; Wu, W.; Shen, H.; Xu, J.; Jiang, Q.; Han, X.; Cai, P. Subdiffraction Imaging of Cleared and Expanded Large-Scale Tissues. *Chem. Biomed. Imaging* **2024**, *2*, 542−559.

(23) Qian, C.; Miao, K.; Lin, L.-E.; Chen, X.; Du, J.; Wei, L. Super-resolution label-free volumetric vibrational imaging. *Nat. Commun.* **2021**, *12*, 3648.

(24) Lin, L.-E.; Miao, K.; Qian, C.; Wei, L. High spatial-resolution imaging of label-free in vivo protein aggregates by VISTA. *Analyst* **2021**, *146*, 4135−4145.

(25) Miao, K.; Lin, L.-E.; Qian, C.; Wei, L. Label-free Super-resolution Imaging Enabled by Vibrational Imaging of Swelled Tissue and Analysis. *J. Vis. Exp.* **2022**, *183*, e63824.

(26) Shi, L.; Klimas, A.; Gallagher, B.; Cheng, Z.; Fu, F.; Wijesekara, P.; Miao, Y.; Ren, X.; Zhao, Y.; Min, W. Super-Resolution Vibrational Imaging Using Expansion Stimulated Raman Scattering Microscopy. *Adv. Sci.* **2022**, *9* (20), e2200315.

(27) Wei, M.; Shi, L.; Shen, Y.; Zhao, Z.; Guzman, A.; Kaufman, L. J.; Wei, L.; Min, W. Volumetric chemical imaging by clearing-enhanced stimulated Raman scattering microscopy. *Proc. Natl. Acad. Sci. U.S.A.* **2019**, *116*, 6608−6617.

(28) Fu, D.; Xie, X. S. Reliable Cell Segmentation Based on Spectral Phasor Analysis of Hyperspectral Stimulated Raman Scattering Imaging Data. *Anal. Chem.* **2014**, *86*, 4115−4119.

(29) Shi, L.; Wei, M.; Miao, Y.; Qian, N.; Shi, L.; Singer, R. A.; Benninger, R. K. P.; Min, W. Highly-multiplexed volumetric mapping with Raman dye imaging and tissue clearing. *Nat. Biotechnol.* **2022**, *40*, 364−373.

(30) Sage, D.; Donati, L.; Soulez, F.; Fortun, D.; Schmit, G.; Seitz, A.; Guiet, R.; Vonesch, C.; Unser, M. DeconvolutionLab2: An open-source software for deconvolution microscopy. *Methods* **2017**, *115*, 28−41.

(31) Jang, H.; Li, Y.; Fung, A. A.; Bagheri, P.; Hoang, K.; Skowronska-Krawczyk, D.; Chen, X.; Wu, J. Y.; Bintu, B.; Shi, L. Super-resolution SRS microscopy with A-PoD. *Nat. Methods* **2023**, *20*, 448−458.

(32) Jang, H.; Li, Y.; Wu, S.; Shi, L. Super-Resolution Stimulated Raman Scattering Microscopy with Graphical User Interface-Supported A-PoD. *Curr. Protoc.* **2024**, *4*, e970.

(33) Gong, L.; Lin, S.; Huang, Z. Super-resolution stimulated Raman scattering microscopy enhanced by quantum light and deconvolution. *Opt. Lett.* **2023**, *48*, 6516−6519.

(34) Varoquaux, G.; Cheplygina, V. Machine learning for medical imaging: methodological failures and recommendations for the future. *NPJ. Digit. Med.* **2022**, *5*, 48.

(35) Lelek, M.; Gyparaki, M. T.; Beliu, G.; Schueder, F.; Griffié, J.; Manley, S.; Jungmann, R.; Sauer, M.; Lakadamyali, M.; Zimmer, C. Single-molecule localization microscopy. *Nat. Rev. Methods Primers* **2021**, *1*, 39.

(36) Shou, J.; Komazawa, A.; Wachi, Y.; Kawatani, M.; Fujioka, H.; Spratt, S. J.; Mizuguchi, T.; Oguchi, K.; Akaboshi, H.; Obata, F.; Tachibana, R.; Yasunaga, S.; Mita, Y.; Misawa, Y.; Kojima, R.; Urano,

Y.; Kamiya, M.; Ozeki, Y. Super-resolution vibrational imaging based on photoswitchable Raman probe. *Sci. Adv.* **2023**, *9*, eade9118.
(37) Shou, J.; Ozeki, Y. Photoswitchable stimulated Raman scattering spectroscopy and microscopy. *Opt. Lett.* **2021**, *46*, 2176−2179.
(38) Tipping, W. J.; Lee, M.; Serrels, A.; Brunton, V. G.; Hulme, A. N. Stimulated Raman scattering microscopy: an emerging tool for drug discovery. *Chem. Soc. Rev.* **2016**, *45*, 2075−2089.
(39) Ao, J.; Fang, X.; Miao, X.; Ling, J.; Kang, H.; Park, S.; Wu, C.; Ji, M. Switchable stimulated Raman scattering microscopy with photochromic vibrational probes. *Nat. Commun.* **2021**, *12*, 3089.
(40) Ao, J.; Fang, X.; Ma, L.; Liu, Z.; Wu, S.; Wu, C.; Ji, M. J. A. P. Photoswitchable vibrational nanoscopy with sub-100-nm optical resolution. *Adv. Photon.* **2023**, *5*, 066001.
(41) Hu, F.; Zeng, C.; Long, R.; Miao, Y.; Wei, L.; Xu, Q.; Min, W. Supermultiplexed optical imaging and barcoding with engineered polyynes. *Nat. Methods* **2018**, *15*, 194.
(42) Yang, Y.; Bai, X.; Hu, F. Photoswitchable polyynes for multiplexed stimulated Raman scattering microscopy with reversible light control. *Nat. Commun.* **2024**, *15*, 2578.
(43) Lee, D.; Qian, C.; Wang, H.; Li, L.; Miao, K.; Du, J.; Shcherbakova, D. M.; Verkhusha, V. V.; Wang, L. V.; Wei, L. Toward photoswitchable electronic pre-resonance stimulated Raman probes. *J. Chem. Phys.* **2021**, *154*, 135102.
(44) Du, J.; Wei, L. Multicolor Photoactivatable Raman Probes for Subcellular Imaging and Tracking by Cyclopropenone Caging. *J. Am. Chem. Soc.* **2022**, *144*, 777−786.
(45) Wilson, L. T.; Tipping, W. J.; Wetherill, C.; Henley, Z.; Faulds, K.; Graham, D.; Mackay, S. P.; Tomkinson, N. C. O. Mitokyne: A Ratiometric Raman Probe for Mitochondrial pH. *Anal. Chem.* **2021**, *93*, 12786−12792.
(46) Manifold, B.; Men, S.; Hu, R.; Fu, D. A versatile deep learning architecture for classification and label-free prediction of hyperspectral images. *Nat. Mach. Intell.* **2021**, *3*, 306−315.
(47) Chadha, R. S.; Guerrero, J. A.; Wei, L.; Sanchez, L. M. Seeing is Believing: Developing Multimodal Metabolic Insights at the Molecular Level. *ACS Cent. Sci.* **2024**, *10*, 758−774.
(48) Zhu, Y.; Ge, X.; Ni, H.; Yin, J.; Lin, H.; Wang, L.; Tan, Y.; Prabhu Dessai, C. V.; Li, Y.; Teng, X.; Cheng, J.-X. Stimulated Raman photothermal microscopy toward ultrasensitive chemical imaging. *Sci. Adv.* **2023**, *9*, eadi2181.

https://doi.org/10.1021/cbmi.4c00057
Chem. Biomed. Imaging XXXX, XXX, XXX−XXX